

Electronic Supplementary Material

Construction of NiCo₂O₄ nanoflake arrays on cellulose-derived carbon nanofibers as a freestanding electrode for high-performance supercapacitors

Xuepeng Ni¹, Kunming Li¹, Changlei Li³, Qianqian Wu¹, Chenglin Liu¹, Huifang Chen^{1,2}, Qilin Wu^{1,2}, Anqi Ju (✉)^{1,2}

1 College of Materials Science and Engineering & State Key Laboratory for Modification of Chemical Fibers and Polymer Materials, Donghua University, Shanghai 201620, China

2 Key Laboratory of High-Performance Fibers & Products, Ministry of Education, Donghua University, Shanghai 201620, China

3 Weifang Xinlong Biomaterial Co., Ltd., Weifang 261000, China

E-mail: anqiju@163.com

Materials

All the materials were used as received in this work. The α -Cellulose (partical size $\sim 25 \mu\text{m}$), polyethylene oxide (PEO), trifluoroacetic acid (TFA), nickel nitrate hexahydrate ($\text{Ni}(\text{NO}_3)_2 \cdot 6\text{H}_2\text{O}$), cobaltous nitrate hexahydrate ($\text{Co}(\text{NO}_3)_2 \cdot 6\text{H}_2\text{O}$), hexamethylenetetramine (HMTA) and polyvinyl alcohol (PVA, 1788) were purchased from Shanghai Macklin Biochemical Technology Co., Ltd. Potassium hydroxide (KOH) was received from Sinopharm Chemical Reagent Co., Ltd. Dichloromethane (DCM) was purchased from Shanghai Lingfeng Chemical Reagent Co., Ltd. Methanol was obtained from Yonghua Chemical Technology (Jiangsu) Co., Ltd. The poly(acrylonitrile-*co*-methylhydrogen itaconate) [P(AN-*co*-MHI)] copolymer was synthesized in our previous work [1], which was used as precursor to prepare carbon nanofibers.

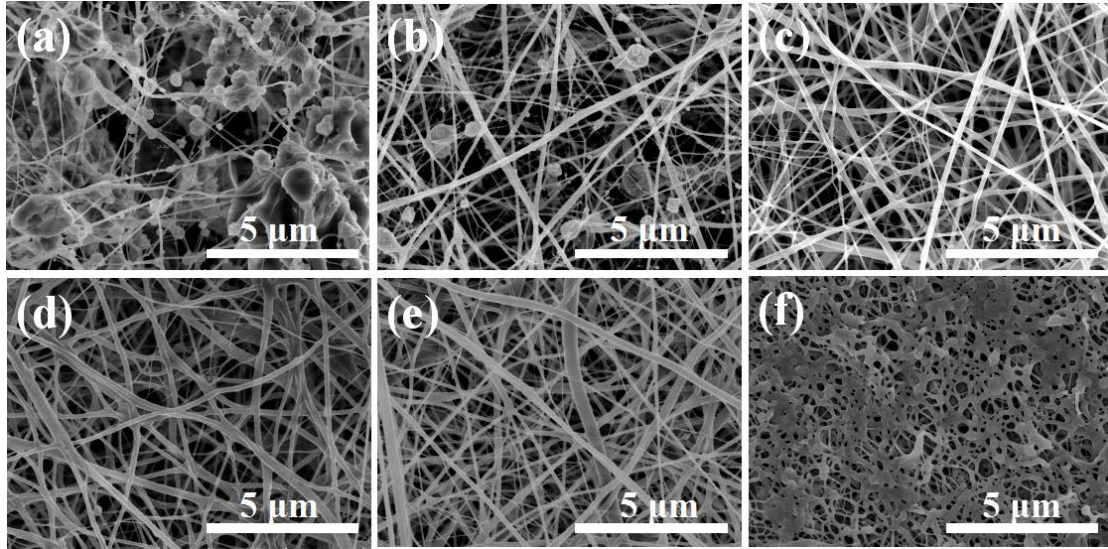


Fig. S1. SEM images of C-NFs prepared at different spinning concentrations (a) 3.5 wt%; (b) 4.5 wt%; (c) 5.5 wt%; (d) 6 wt%; (e) 6.5 wt %; (f) 7 wt%.

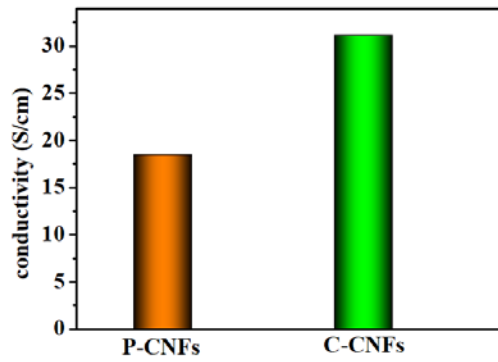


Fig. S2. The conductivity of C-CNFs and P-CNFs at 1600°C.

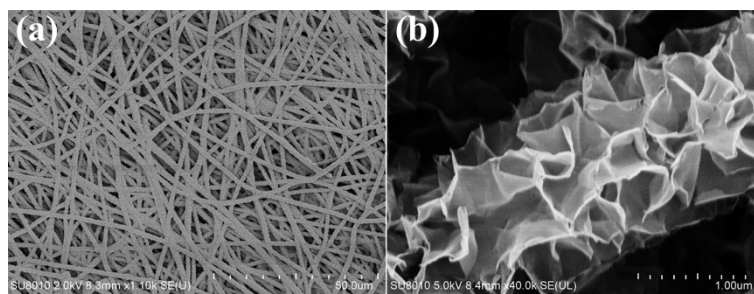


Fig. S3. SEM images of P-CNFs/NiCo₂O₄ electrode materials after calcination.

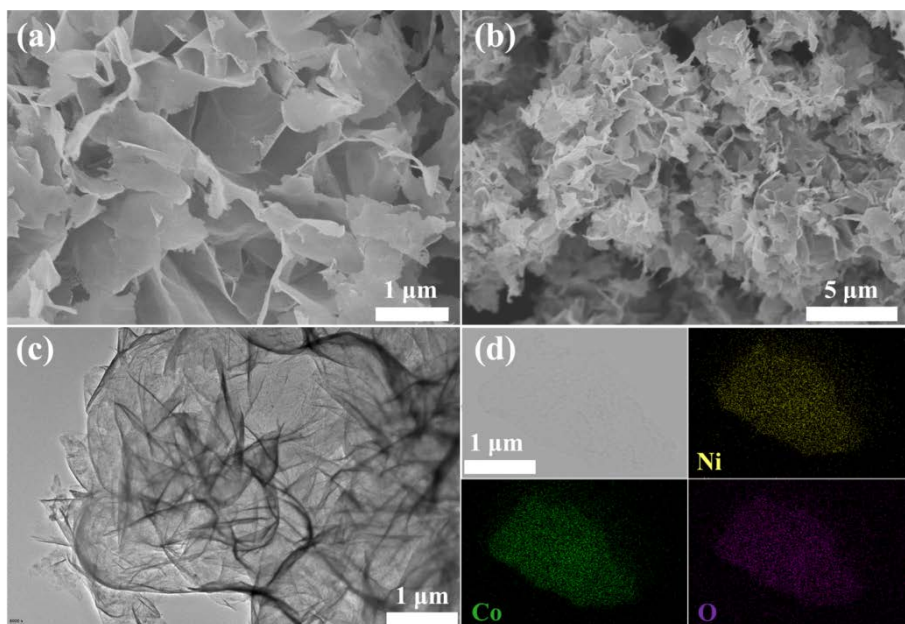


Fig. S4. SEM images (a-b), TEM images (c) and elemental mapping for Ni, Co and O (d) of bare NiCo_2O_4 .

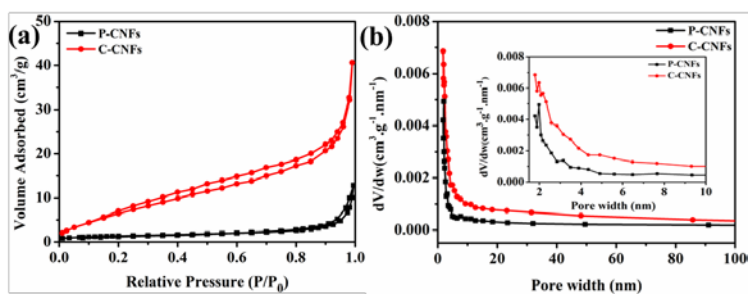


Fig. S5. N_2 adsorption-desorption isotherms (a) and pore size distribution curves (b and inset) of P-CNFs and C-CNFs.

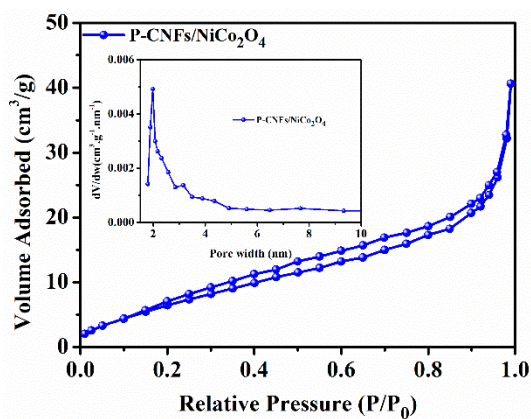


Fig. S6. N_2 adsorption-desorption isotherms and pore size distribution curves (inset) of P-CNFs/ NiCo_2O_4 nanoflake arrays.

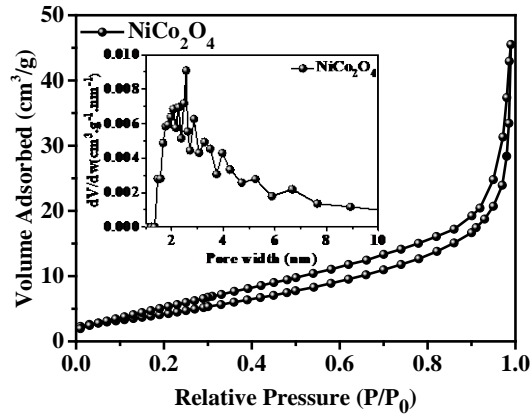


Fig. S7. The N_2 adsorption-desorption isotherms and pore size distribution curves of bare $NiCo_2O_4$.

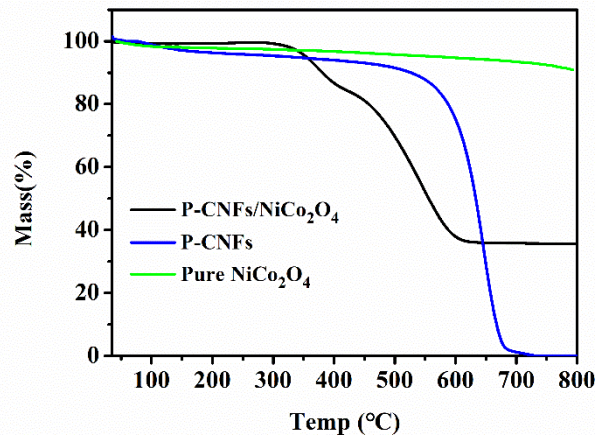


Fig. S8. TG patterns of P-CNFs/ $NiCo_2O_4$ nanoflake arrays, P-CNFs and pure $NiCo_2O_4$.

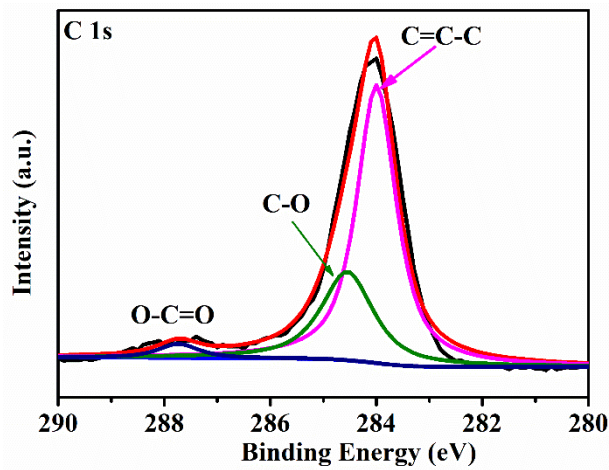


Fig. S9. High-resolution XPS spectra for C 1s.

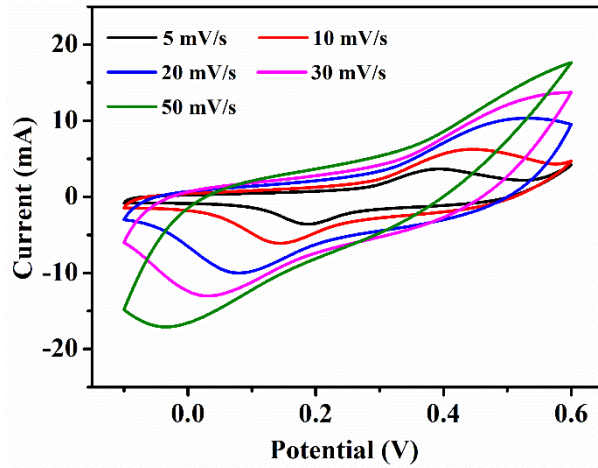


Fig. S10. CV curves of P-CNFs/NiCo₂O₄ nanoflake arrays at different scan rates.

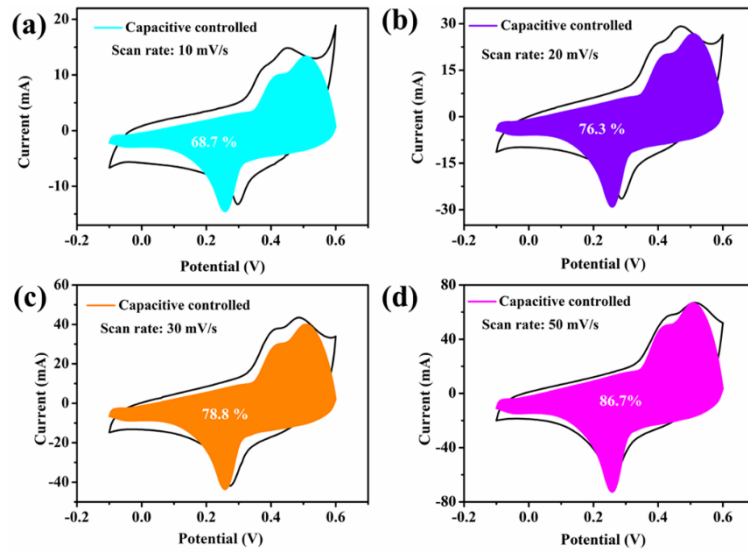


Fig. S11. The capacitive controlled contribution of C-CNFs/NiCo₂O₄ nanoflake arrays at different scan rates.

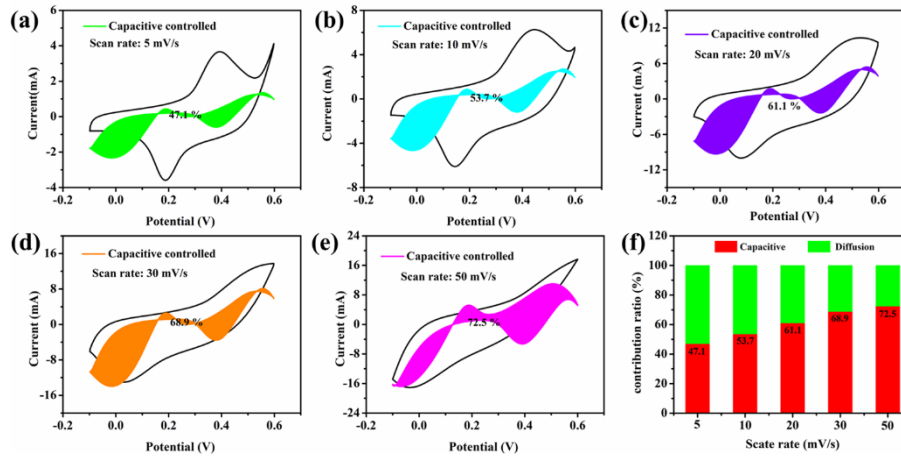


Fig. S12. The capacitive controlled contribution and contribution comparison of P-CNFs/NiCo₂O₄ nanoflake arrays at different scan rates.

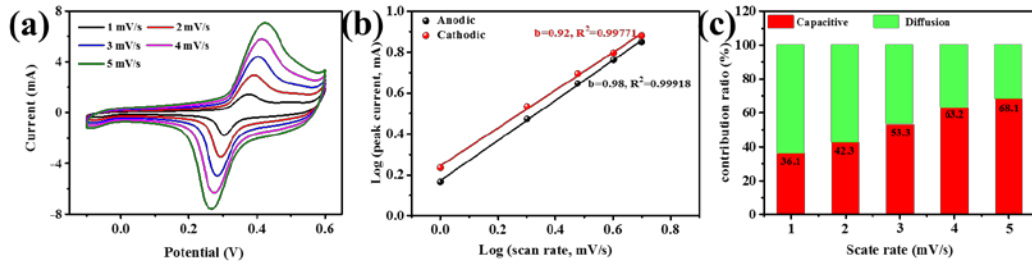


Fig. S13. (a) The CV curves at various scan rates ranging from 1 mV/s to 5 mV/s and (b) logarithm relationship between anodic/ cathodic peaks current and scan rate of C-CNFs/NiCo₂O₄ nanoflake arrays; (c) the contribution comparison at different scan rates of C-CNFs/NiCo₂O₄ nanoflake arrays.

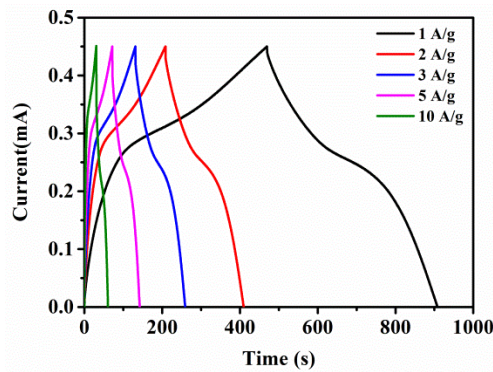


Fig. S14. Galvanostatic charge-discharge curves of P-CNFs/NiCo₂O₄ nanoflake arrays at different current densities.

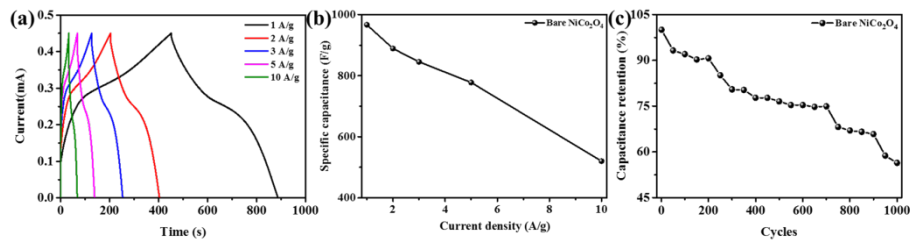


Fig. S15. The GCD curves (a), specific capacitance (b) at various current densities and long-cycling performances at 10 A/g (c) of bare NiCo₂O₄.

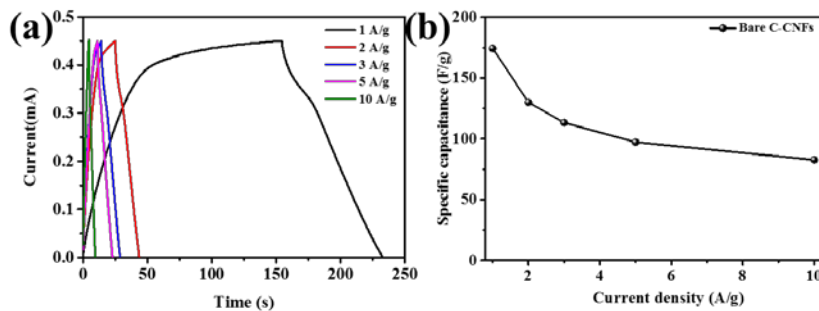


Fig. S16. The GCD curves (a), specific capacitance (b) at various current densities of bare C-CNFs.

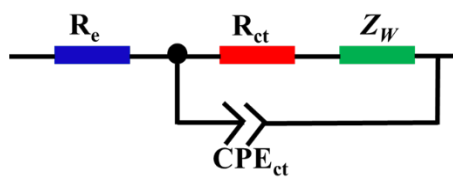


Fig. S17. The equivalent circuit of C-CNFs/NiCo₂O₄ and P-CNFs/NiCo₂O₄ nanoflake arrays.

Table S1 The carbon content of C-CNFs with different temperature.

Temperature (°C)	C (%)	H (%)	N (%)
800	88.38	1.55	0.05
1200	90.74	0.59	0.75
1600	98.76	0.36	0.16

[1] A. Ju, S. Guang, H. Xu, Effect of comonomer structure on the stabilization and spinnability of polyacrylonitrile copolymers, Carbon 54 (2013) 323-335.